

## Numerical study of performance optimization in a proton exchange membrane fuel cell

Chang-Ming Ling<sup>1</sup>, Chun-Hua Min<sup>2</sup>, Xiao-Long Ruan<sup>1</sup>, Zhang-Jing Zheng<sup>1</sup>

<sup>1</sup> School of Engineering  
Guangdong Ocean University  
Zhanjiang, 524025 (P R China)  
Mobile number:+0086 13828267162, e-mail: ling-cm@163.com

<sup>2</sup> School of Energy and Environmental Engineering  
Hebei University of Technology  
Tianjin, 300401, (P R China)  
e-mail: chmin@hebut.edu.cn

**Abstract.** Some parameters such as  $i_{a,ref}$ ,  $c_{H,ref}$ ,  $i_{c,ref}$ ,  $c_{O,ref}$ ,  $\alpha_a$  and  $\alpha_c$  that affect the PEMFC performance are numerically studied in the present work. To reveal the effects of the above parameters on the cell performance, several parameter groups have been presented. The results show that different parameter values may result in a wholly identical polarization curve when the parameters agree with a given function. The function indicates the effects of several parameters and can be used to direct the optimization of PEMFC performance.

### Key words

Proton exchange membrane fuel cell; Parameter; Numerical analysis; Polarization curve; Optimization

### 1. Introduction

The proton exchange membrane fuel cell (PEMFC) is considered to be a promising power source, especially for transportation and stationary cogeneration applications due to its high efficiency, low-temperature operation, high power density, fast startup, and system robustness. Recently, many computational models have been developed and published to reveal the fundamental transport phenomena taking place in the PEMFC and to optimize the PEMFC performance. There are many parameters that affect the PEMFC performance which have been studied by many researchers. Stockie et al. [1] performed a sensitivity study of a PEMFC model. It was found that the PEMFC performance is obviously affected by some parameters. Chan and Tun [2] developed a model of catalyst layer and investigated the effects of the cathode reference exchange current density, reference oxygen concentration, oxygen diffusivity and catalyst layer porosity on PEMFC performance. Lum and McGurik [3] developed a model of the cathode of a PEMFC with an

inter-digitated gas distributor with the intention of studying the effects of various parameters such as electrode permeability, thickness and shoulder width. Al-Baghdadi and Al-Janabi [4] developed a three-dimensional model of a PEMFC to investigate the effects of various parameters such as proton exchange membrane thickness, diffusion layer porosity, diffusion layer thermal conductivity on the fuel cell performance. Chu et al. [5] investigated the porosity of gas diffusion layer (GDL) of a PEMFC. The results showed that a non-uniform porosity of GDL is necessary to improve the performance. Du et al. [6] investigated the effects of the effective proton and electronic conductivity of the catalyst layers on PEMFC performance. Crujicic et al. [7] performed a sensitivity analysis to determine the effect of six parameters on a PEMFC performance. The results showed that, while the predicted average current density at the membrane/cathode interface is affected by uncertainties in a number of model parameters, the optimal designs of the PEM cathode and the interdigitated air distributor are quite robust. Wu et al. [8] also found some operating parameters have strong impacts on the PEMFC performance. Min et al. [9] investigated the influence of some parameters on the performance. They classified the parameters according to their influence on the fuel cell as: insensitive, sensitive, and highly sensitive. Furthermore, they found that different parameter values may result in a nearly identical polarization curve of a PEMFC, and hence they concluded that polarization curve only is insufficient to validate the PEMFC model.

The present work focused on the effects of six parameters on the PEMFC performance. Some functions formed by several parameters were presented to indicate the effects.

## 2. Model description

A schematic view of a PEMFC with parallel flow fields and computational domain is shown in Fig. 1. It is assumed that the PEMFC structure is repeated periodically along the y-direction. To save computational time, a typical unit shown in the figure is taken as the computational domain. Humidified hydrogen is fed into the anode channel, whereas dry is fed into the cathode channel.

The assumptions adopted in the present model are as follows:

- (1) The fuel cell operates under steady-state condition;
- (2) The gas mixture is an incompressible ideal fluid;
- (3) The gas flow in the channels is laminar;
- (4) All the porous zones in the fuel cell domain are assumed to be isotropic and homogeneous, and the membrane is considered impervious to reactant gases; and
- (5) The gas and liquid phases in the fuel cell exist as continuous phases.

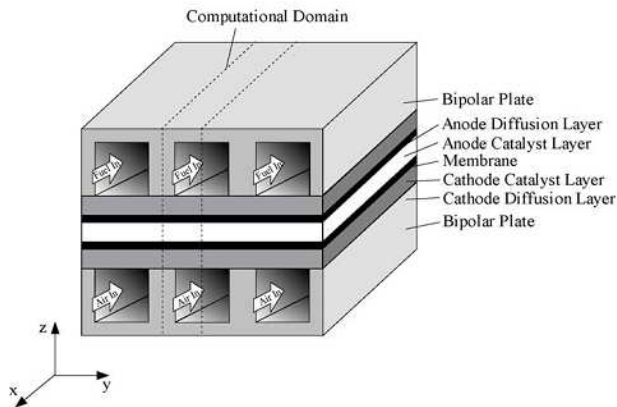


Fig.1. Schematic view of a PEMFC

### A. Governing equations

The three-dimensional, two-phase, non-isothermal model consists of non-linear, coupled partial differential equations which represent the conservation of mass, momentum, species, charge and energy. The conservation equations are described in the vector form as follows.

(1) Mass conservation equation:

$$\nabla \cdot (\epsilon \rho \bar{u}) = S_m \quad (1)$$

(2) Momentum conservation equation:

$$\nabla \cdot (\epsilon \rho \bar{u} \bar{u}) = -\epsilon \nabla p + \nabla \cdot (\epsilon \mu \nabla \bar{u}) + S_u \quad (2)$$

(3) Energy conservation equation:

$$\nabla \cdot (\epsilon \rho c_p \bar{u} T) = \nabla \cdot (k_{\text{eff}} \nabla T) + S_Q \quad (3)$$

(4) Species conservation equation:

$$\nabla \cdot (\epsilon \bar{u} C_k) = \nabla \cdot (D_{k,\text{eff}} \nabla C_k) + S_k \quad (4)$$

(5) Electrical current density is given by Butler-Volmer equation:

$$i_a = i_{a,\text{ref}} \left( \frac{C_h}{C_{h,\text{ref}}} \right)^{\frac{1}{2}} \left\{ \exp\left[ \frac{\alpha_a F}{RT} \eta_a \right] - \exp\left[ -\frac{(1-\alpha_a)F}{RT} \eta_a \right] \right\} \quad (5)$$

$$i_c = i_{c,\text{ref}} \left( \frac{C_o}{C_{o,\text{ref}}} \right)^{\frac{1}{2}} \left\{ \exp\left[ \frac{\alpha_c F}{RT} \eta_c \right] - \exp\left[ -\frac{(1-\alpha_c)F}{RT} \eta_c \right] \right\} \quad (6)$$

(6) Electrical charge equations:

$$\nabla \cdot (\kappa_s \nabla \phi_s) + S_s = 0 \quad (7)$$

$$\nabla \cdot (\kappa_m \nabla \phi_m) + S_m = 0 \quad (8)$$

(7) Liquid saturation equation:

$$\frac{\partial(\epsilon \rho_l s)}{\partial t} + \nabla \cdot (\rho_l \frac{K s^3}{\mu_l} \frac{dp_c}{ds} \nabla s) = r_w \quad (9)$$

In the above equations, the subscript “l” stands for the liquid phase and “s” for the solid phase. Different species are denoted by the subscript “k”, “w” is for water; “h” and “o” are for hydrogen and oxygen respectively. Cathode side and anode side properties are denoted by the subscript “c” and “a” respectively.

Table I. - Model parameters for basic case

No.	Parameter	Symbol	Unit	Value
1	Gas channel length	$L_{\text{ch}}$	m	0.05
2	Gas channel width	$W_{\text{ch}}$	m	$1 \times 10^{-3}$
3	Ribbed area width	$W_{\text{cc}}$	m	$1 \times 10^{-3}$
4	Bipolar plate base height	$H_{\text{cc}}$	m	$5 \times 10^{-4}$
5	Gas channel height	$H_{\text{ch}}$	m	$1 \times 10^{-4}$
6	Diffusion layer height	$H_{\text{d}}$	m	$2.6 \times 10^{-4}$
7	Catalyst layer height	$H_{\text{ct}}$	m	$1 \times 10^{-5}$
8	Membrane height	$H_{\text{m}}$	m	$2.3 \times 10^{-4}$
9	Gas channel inlet temperature	$T_{\text{in}}$	K	353
10	Anode reference exchange current density	$i_{a,\text{ref}}$	$\frac{\text{A}}{\text{m}^2}$	$9.23 \times 10^8$
11	Cathode reference exchange current density	$i_{c,\text{ref}}$	$\frac{\text{A}}{\text{m}^2}$	$1.05 \times 10^6$
12	Porosity of diffusion layer	$\epsilon_{\text{d}}$		0.4
13	Porosity of catalyst layer	$\epsilon_{\text{ct}}$		0.4
14	Absolute permeability	$K$	$\text{m}^2$	$2 \times 10^{-11}$

Boundary conditions have to be applied for all variables of interest in computational domain.

In order to reduce computational cost, advantage is taken of the geometric periodicity which is shown in Fig. 1. At the gas channel entries, such as gas mixture velocities, pressure, temperature and component concentrations, are specified. At the outlets of the gas flow channels, only the pressure is prescribed as the desired electrode pressure; for other variables, the gradient in the flow direction is assumed to be zero. Since the fluid channels are contacted with the collector plates, no boundary conditions have to be prescribed here. Conjugate heat transfer, impermeability and no-slip conditions are applied to solid-fluid interfaces within the domain.

## B. Solution algorithm

The commercial computational fluid dynamic software Fluent (version 6.3) is used to solve the PEMFC model. The SIMPLEX algorithm is utilized to deal with the coupling of the velocity and pressure.

## 3. Results and discussion

### A. Model validation

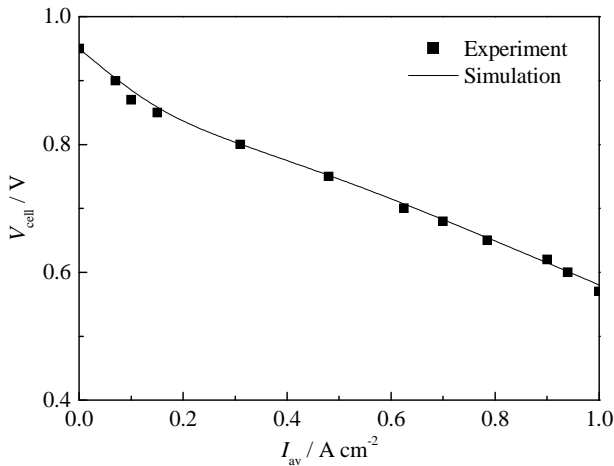


Fig. 2. Polarization curves of simulation and experiment

The model results are compared with the experimental results of Ticianelli et al. [10] as shown in Fig. 2. It can be seen that the model results agree very well with that of experimental results.

### B. Effects of the parameters on the PEMFC performance

Table II. - Parameters used in the present model

Parameters	Symb ol	Unit	Range	Refer nces
Anode transfer coefficient	$\alpha_a$		0.5–2.0	[11,12 ]
Cathode transfer coefficient	$\alpha_c$		0.8–3.75	[13,14 ]
Anode reference exchange current density	$i_{a,ref}$	$A\ m^{-3}$	$5.0 \times 10^8$ – $1.4 \times 10^{11}$	[15,16 ]
Cathode reference exchange current density	$i_{c,ref}$	$A\ m^{-3}$	$10$ – $1.0 \times 10^7$	[17,18 ]
Reference hydrogen concentration	$C_{H,ref}$	$\frac{mol}{m^3}$	26.6–56.4	[19,17 ]
Reference oxygen concentration	$C_{O,ref}$	$\frac{mol}{m^3}$	1.2–40.88	[14,20 ]

The effects of the parameters on the PEMFC performance are very complicated because the parameters may affect each other. To simplify the discussion, there are six parameters are investigated in the present work and are listed in table 2, where the parameter values and variation ranges in the literature are also shown. In addition, the

original literatures that gave the upper and lower limits of the parameter values are also provided. It can be seen that these parameter values vary in a large range. To reveal the relationship of the parameters, the polarization curves of the PEMFC are assumed unchangeable under different parameter values.

#### 1) Effect of $i_{a,ref}$ and $C_{H,ref}$ on the cell performance

The effects of  $i_{a,ref}$  and  $C_{H,ref}$  on the cell performance is firstly discussed. To simplify Eq. (5), we define

$$i_a = A_1 c_H^{\frac{1}{2}}, \quad B_1 = F\eta_a / RT, \quad M_1 = (e^{B_1\alpha_a} - e^{B_1\alpha_c}) / A_1$$

where,  $A_1$ ,  $B_1$  and  $M_1$  are assumed constants. Substituting these into Eq. (5) yield

$$M_1 = \frac{(C_{H,ref})^{\frac{1}{2}}}{i_{a,ref}} \quad (10)$$

The above equation means the polarization curves of the PEMFC will be unchangeable if  $i_{a,ref}$  and  $C_{H,ref}$  agree with Eq. (10). Figure 3 shows the effects of  $i_{a,ref}$  and  $C_{H,ref}$  on the PEMFC performance when  $M_1=4.5 \times 10^{-9}$ . It can be seen that the polarization curves at different  $i_{a,ref}$  and  $C_{H,ref}$  are wholly identical. Figure 4 shows the effect of  $M_1$  on the cell performance. It can be seen that the higher of  $M_1$  is beneficial to improve the cell performance.

It should be noted that  $A_1$  and  $B_1$  are assumed constants in the above deduction. In fact, it is very difficult to be satisfied because anode current density is nonlinear to hydrogen concentration and  $\eta_a$  is not a constant. However, if only  $M_1$  remains constant, the polarization curves of the PEMFC will be unchangeable even if  $A_1$  and  $B_1$  are not constants. Hence,  $M_1$  can be used to reveal the effects of  $i_{a,ref}$  and  $C_{H,ref}$  on the cell performance and to optimize the cell performance. In fact, the following sections have the similar conclusion with the above analysis.

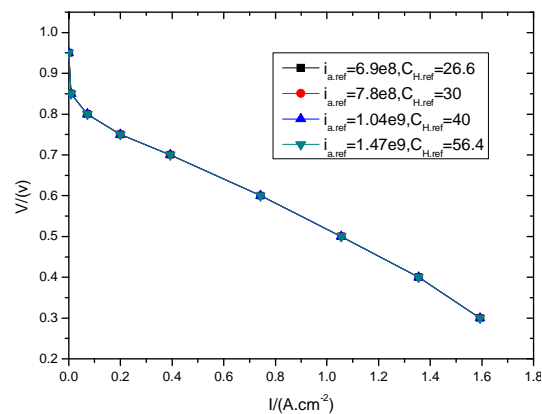


Fig. 3. An identical porization curve with different values of  $i_{a,ref}$  and  $C_{H,ref}$  when  $M_1=4.5 \times 10^{-9}$

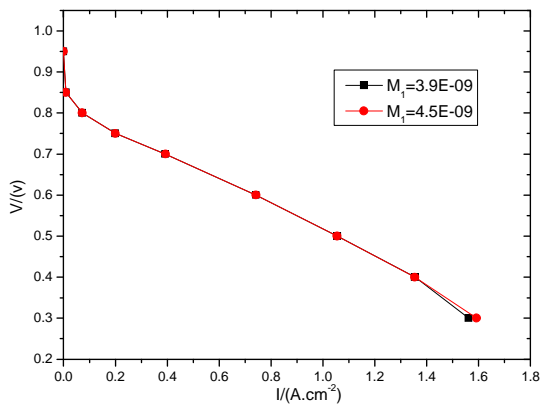


Fig. 4. Effect of  $M_1$  on the cell performance

### 2) Effects of $i_{c,ref}$ and $C_{O,ref}$ on the cell performance

Using the above method, we define

$$i_c = A_2 c_H, \quad B_2 = F\eta_c / RT, \quad M_2 = (e^{-B_2\alpha_a} - e^{B_2\alpha_c}) / A_2$$

where,  $A_2$ ,  $B_2$  and  $M_2$  are assumed constants. Substituting these into Eq. (6) yield

$$M_2 = \frac{C_{O,ref}}{i_{c,ref}} \quad (11)$$

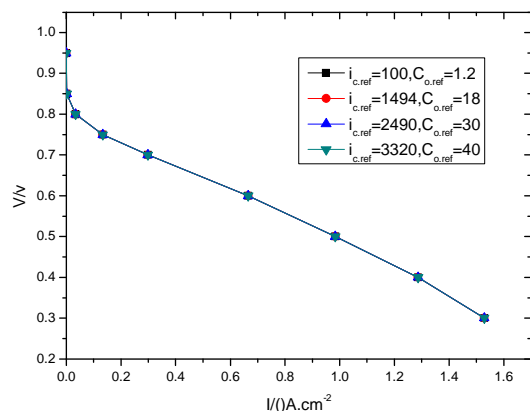


Fig. 5. An identical porization curve with different values of  $i_{c,ref}$  and  $C_{O,ref}$  when  $M_2=1.2 \times 10^{-5}$

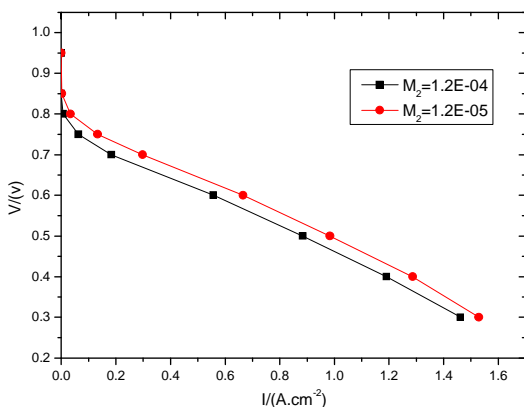


Fig. 6. Effect of  $M_2$  on the cell performance

The above equation means the polarization curves of the PEMFC will be unchangeable if  $i_{c,ref}$  and  $C_{O,ref}$  agree with Eq. (11). Figure 5 shows the effects of  $i_{c,ref}$  and  $C_{O,ref}$  on the PEMFC performance when  $M_2=4.5 \times 10^{-5}$ . It can be seen that the polarization curves at different  $i_{c,ref}$  and  $C_{O,ref}$  are wholly identical. Figure 6 shows the effect of  $M_2$  on the cell performance. It can be seen that  $M_2$  has a significantly effect on the cell performance and the lower of  $M_2$  is beneficial to improve the cell performance.

### 3) Effects of $i_{a,ref}$ and $\alpha_a$ on the cell performance

Now, we define

$$A_3 = i_a (c_H c_{H,ref})^{-\frac{1}{2}} \quad B_3 = F\eta_a / RT$$

where,  $A_3$  and  $B_3$  are assumed constants. Substituting these into Eq. (5) yield

$$i_{a,ref} = A_3 (e^{B_3\alpha_a} - e^{B_3\alpha_c})^{-1} \quad (12)$$

According to Tafel equation, the second expression in the bracket of Eq. (12) is very small and can be neglected. Hence, the following equation can be obtained:

$$i_{a,ref} = A_3 e^{-B_3\alpha_a} \quad (13)$$

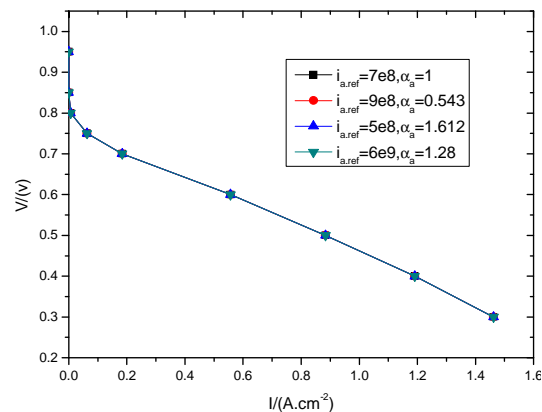


Fig. 7. An identical porization curve with different values of  $i_{a,ref}$  and  $\alpha_a$  when  $A_3=1.2133 \times 10^9$  and  $B_3=-0.55$

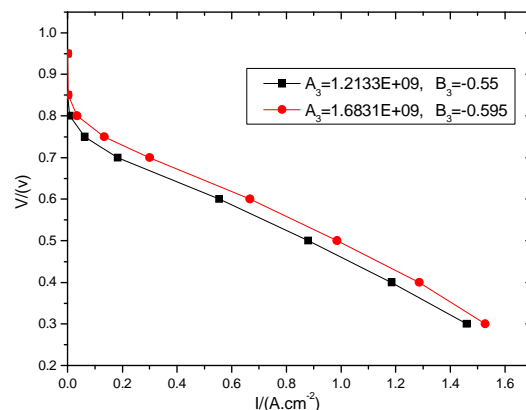


Fig. 8. Effects of  $A_3$  and  $B_3$  on the cell performance

The above equation means the polarization curves of the PEMFC will be unchangeable if  $i_{a,ref}$  and  $\alpha_a$  agree with Eq. (13). Figure 7 shows the effects of  $i_{a,ref}$  and  $\alpha_a$  on the PEMFC performance when  $A_3=1.2133 \times 10^9$  and  $B_3=-0.55$ . It can be seen that the polarization curves are

wholly identical. Figure 8 shows the effects of  $A_3$  and  $B_3$  on the cell performance. It can be seen that  $A_3$  and  $B_3$  strongly affect the cell performance. Furthermore,  $A_3$  and  $B_3$  indicate the effects of  $i_{a,ref}$  and  $\alpha_c$ , respectively, on the cell performance. Hence, Eq. (13) does not simplify the effects of the two parameters on the cell performance. However, it supplies an effective method to analysis the effects. More detailed analyses will be presented in our future work.

#### 4) Effects of $i_{c,ref}$ and $\alpha_c$ on the cell performance

Then, we define

$$A_4 = i_c c_o^{-1} c_{O,ref} \quad B_4 = F\eta_c / RT$$

where,  $A_4$  and  $B_4$  are assumed constants. Substituting these into Eq. (6) yield

$$i_{c,ref} = A_4 e^{B_4 \alpha_c} \quad (14)$$

The above equation means the polarization curves of the PEMFC will be unchangeable if  $i_{c,ref}$  and  $\alpha_c$  agree with Eq. (14). Figure 9 shows the effects of  $i_{c,ref}$  and  $\alpha_c$  on the PEMFC performance when  $A_4=3.4545 \times 10^8$  and  $B_4=-5.3831$ . It can be seen that the polarization curves are nearly identical at higher current density. While at lower current density ( $I_{av} < 0.6 \text{ A cm}^{-2}$ ), there is some difference between the curves. It is due to Eq. (14) that is deduced from Tafel equation, which is a simplification of Butler-Volmer equation. Figure 10 shows the effects of  $A_4$  and  $B_4$  on the cell performance. It can be seen that the effects of  $A_4$  and  $B_4$  on the cell performance are similar to those of  $A_3$  and  $B_3$ . More detailed analysis will not be further presented.

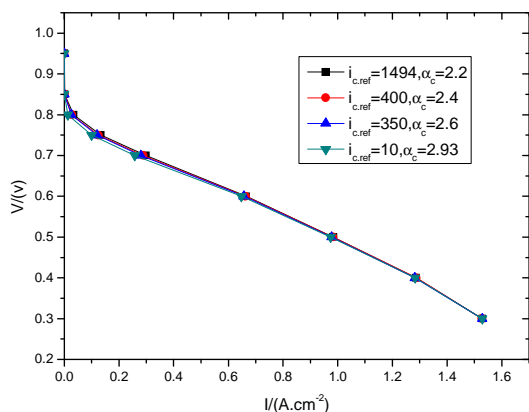


Fig. 9. An identical polarization curve with different values of  $i_{c,ref}$  and  $\alpha_c$  when  $A_3=1.2133 \times 10^9$  and  $B_3=-0.55$

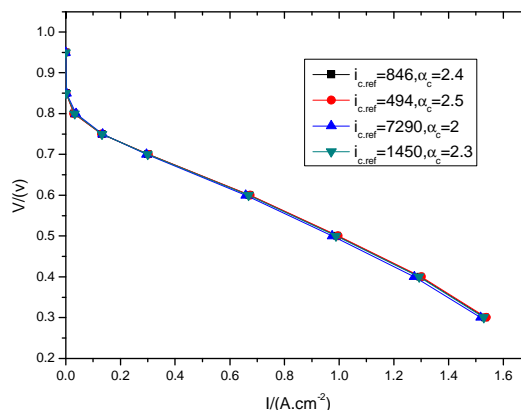


Fig. 10. Effects of  $A_4$  and  $B_4$  on the cell performance

#### 5) Effects of $i_{a,ref}$ , $i_{c,ref}$ , $C_{H,ref}$ and $C_{O,ref}$ on the cell performance

From Eq. (10) and (11) yield

$$M = M_1 M_2 = \frac{C_{H,ref}^{\frac{1}{2}} C_{O,ref}}{i_{a,ref} i_{c,ref}} \quad (15)$$

where  $M$  denotes the effects of  $i_{a,ref}$ ,  $i_{c,ref}$ ,  $C_{H,ref}$

and  $C_{O,ref}$  on the cell performance. However, the polarization curves of the PEMFC may change even the four parameters agree with Eq. (15) as shown in Fig. 11. Hence, it needs other conditions to redefine the four parameters. Meanwhile, Eq. (10) or (11) can be taken as additional conditions to meet the above requirement. Hence,  $M$  and  $M_1$  or  $M$  and  $M_2$  can be used to denote the effects of the four parameters on the cell performance. For instance, Figure 12 shows that four different polarization curves are wholly identical with different values of the four parameters which agree with Eq. (15), Eq. (10) and Eq. (11).

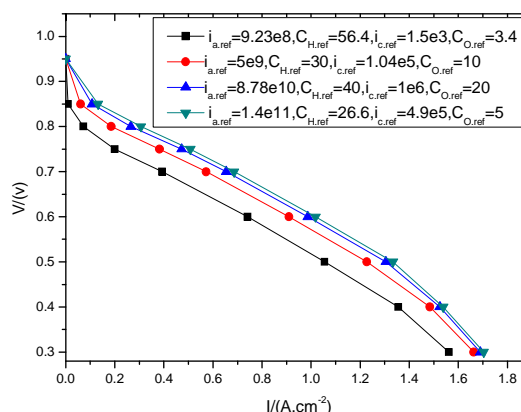


Fig. 11. Effects of four parameters on the cell performance

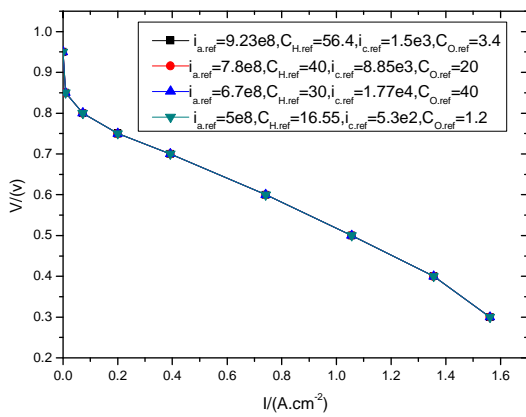


Fig. 12. A polarization curve with different values of the four parameters

## 4. Conclusions

The effects of six parameters on the PEMFC performance have been numerically studied. The main conclusions are:

- (1) The value of  $M_1$  denotes the effects of  $i_{a,ref}$  and  $c_{H,ref}$  on PEMFC performance and can be used to direct the optimization of a PEMFC.
- (2) The value of  $M_2$  denotes the effects of  $i_{c,ref}$  and  $c_{O,ref}$  on PEMFC performance and can be used to direct the optimization of a PEMFC.
- (3) The parameter group of  $M$  and  $M_1$  or  $M$  and  $M_2$  denotes the effects of  $i_{a,ref}$ ,  $c_{H,ref}$ ,  $i_{c,ref}$  and  $c_{O,ref}$  on PEMFC performance. The parameter group supplies a method to optimize PEMFC performance and the more detailed analysis will be presented in our future work.

## References

- [1] J.M. Stockie, K. Promislow, B.R. Wetton, A finite volume method for multicomponent gas transport in a porous fuel cell electrode, *Int. J. Numer. Methods Fluids* 6 (2003) 577–599.
- [2] S.H. Chan, W.A. Tun, Catalyst layer models for proton exchange membrane fuel cells. *Chem. Eng. Technol.* 1 (2001) 51–57.
- [3] K.W. Lum, J.J. McGurik, 2D and 3D modeling of a PEMFC cathode with interdigitated gas distributors, *J. Electrochem. Soc.* 4 (2005) A811–A817.
- [4] M.A.R.S. Al-Baghdadi, H.A.K.S. Al-Janabi. Modeling optimizes PEM fuel cell performance using three-dimensional multi-phase computational fluid dynamics model, *Energy Conversion and Management* 48 (2007) 3102–3119.
- [5] H.S. Chu, C. Yeh, F. Chen, Effects of porosity change of gas diffuser on performance of proton exchange membrane fuel cell, *J. Power Sources* 1 (2003) 1–9.
- [6] C.Y. Du, P.F. Shi, X.Q. Cheng, et al, Effective protonic and electronic conductivity of the catalyst layers in proton exchange membrane fuel cells, *Electrochem. Commun.* 5 (2004) 435–440.
- [7] M. Grujicic, C.L. Zhao, K.M. Chittajallu, et al, Cathode and interdigitated air distributor geometry optimization in polymer electrolyte membrane (PEM) fuel cells, *Mater. Sci. Eng. B* 3 (2004) 241–252.
- [8] S.J. Wu, S.W. Shiah, W.L. Yu, Parametric analysis of proton exchange membrane fuel cell performance by using the Taguchi method and a neural network, *Renewable Energy* 1(2009) 35–144
- [9] C.H. Min, Y.L. He, X.L. Liu, et al, Parameter sensitivity examination and discussion of PEM fuel cell simulation model validation Part II: results of sensitivity analysis and validation of the model, *J. Power Sources* 1 (2006) 374–385.
- [10] E.A. Ticianelli, C.R. Derouin, S. Srinivasan, Localization of platinum in low catalyst loading electrodes to attain high power densities in SPE fuel cells, *J. Electrochem. Soc.* 251 (1988) 275–295.
- [11] T. Berning, D.M. Lu, N. Djilali, Three-dimensional computational analysis of transport phenomena in a PEM fuel cell, *J. Power Sources* 1–2(2002) 284–294.
- [12] T.C. Jen, T. Yan, S.H. Chan, Chemical reacting transport phenomena in a PEM fuel cell, *Int. J. Heat Mass Transfer* 22 (2003) 4157–4168.
- [13] A.A. Kulikovskiy, Quasi-3D modeling of water transport in polymer electrolyte fuel cells, *J. Electrochem. Soc.* 11 (2003) A1432–A1439.
- [14] Q. Wang, M. Eikerling, D. Song, et al, Functionally graded cathode catalyst layers for polymer electrolyte fuel cells. I. Theoretical modeling, *J. Electrochem. Soc.* 7(2004) A950–A957.
- [15] T.H. Zhou, H.T. Liu, A 3D model for PEM fuel cells operated on reformat, *J. Power Sources* 1-2 (2004) 101–110.
- [16] K.V. Zhukovskiy, Three dimensional model of oxygen transport in a porous diffuser of a PEM fuel cell, *AIChE J.* 12 (2003) 3029–3036.
- [17] D.M. Bernardi, M.W. Verbrugge, A mathematical model of the solid-polymer-electrolyte fuel cell, *J. Electrochem. Soc.* 9 (1992) 2477–2491.
- [18] M. Wöhr, K. Bolwin, W. Schnurnberger, et al, Dynamic modeling and simulation of a polymer membrane fuel cell including mass transport limitation, *Int. J. Hydrogen Energy* 3 (1998) 213–218.
- [19] N.P. Siegel, M.W. Ellis, D.J. Nelson, et al, A two-dimensional computational model of a PEMFC with liquid water transport, *J. Power Sources* 2 (2004) 173–184.
- [20] H. Ju, H. Meng, C.Y. Wang, A single-phase, non-isothermal model for PEM fuel cells, *Int. J. Heat Mass Transfer* 7 (2005) 1303–1315.